

Rate-based Modelling of CO₂ Absorption with Sandwich Packings

Steve Flechsig^a, Johanna Sohr^b, Markus Schubert^c, Uwe Hampel^{b,c}, Eugeny Y. Kenig^{a,*}

^aPaderborn University, Chair of Fluid Process Engineering, Pohlweg 55, 33098 Paderborn/Germany

^bTechnical University Dresden, Institute of Power Engineering, 01069 Dresden/Germany

^cHelmholtz-Zentrum Dresden-Rossendorf, Institute of fluid dynamics, Bautzner Landstrasse 400, 01328 Dresden/Germany
eugen.y.kenig@upb.de

The efficiency of fluid separation processes can be enhanced by the application of sandwich packings (SPs). They consist of two alternating layers of industrially available standard packings with different specific surface areas, one with lower (the so-called holdup layer, HL) and another with higher (the so-called de-entrainment layer, DL) capacity. SPs are typically used at operating conditions between the flooding points of HL and DL. Above the HL, a froth sub-layer is formed, which reveals high separation efficiency due to intensified phase contact. In a collaborative project, the effects of the individual flow regimes on fluid dynamics and mass transfer are being investigated, both experimentally and theoretically. In order to identify the impact of the individual flow regimes, experiments in an absorption/desorption plant are supplemented by flow imaging measurements. This paper focuses on a rate-based model, in which the heterogeneous flow patterns in SPs are considered via appropriate correlations. In order to validate this model, we measured CO₂ absorption characteristics under the influence of different operating and design parameters and compared them with the simulation results.

1. Introduction

Carbon dioxide (CO₂) is one of the most important greenhouse gases, which causes climate change. One of the technologies to reduce CO₂-emissions of coal, oil and gas fired plants is its absorption by aqueous alkanolamine solutions followed by the solvent regeneration. These operations are often performed in counter-current packed columns. However, this process is very energy intensive and leads to high losses of efficiency in fossil-fired power plants. For the reduction of these losses, the progress in the development of column internals is significant, because the internals directly affect the separation efficiency as well as capacity and pressure drop of separation units. A promising way to increase separation efficiency and capacity of packed columns is the application of sandwich packings (SPs).

These packings consist of two alternating layers of industrially available standard packings with different specific surface areas. Consequently, the holdup layer (HL) has lower loading limits compared to those of the de-entrainment layer (DL). In the operating region between the flooding points of the two layers, flow regimes typical for either structured packings or trays can be met within a SP element. Above the flooded HL, a froth sub-layer is formed. In the upper section of the DL, film-like flow patterns can be observed. Furthermore, the entrainment from the froth is captured by the DL (Kashani et al., 2005).

Due to the heterogeneous flow pattern, pressure drop and holdup of SPs show a special behaviour. A comparison of pressure drop and holdup characteristics of SPs with those of conventional packings is given in Figure 1. It is shown that the characteristic pressure drop, holdup and the loading limits of SPs could be derived from those of structured packings, in the way illustrated in Figures 1c and 1d. However, the gas load at the flooding point of the DL is shifted to lower values. Besides, it was found that an additional pressure drop and an additional holdup arise because of the developed froth layer after reaching the flooding point of the HL (Flechsig et al., 2016).

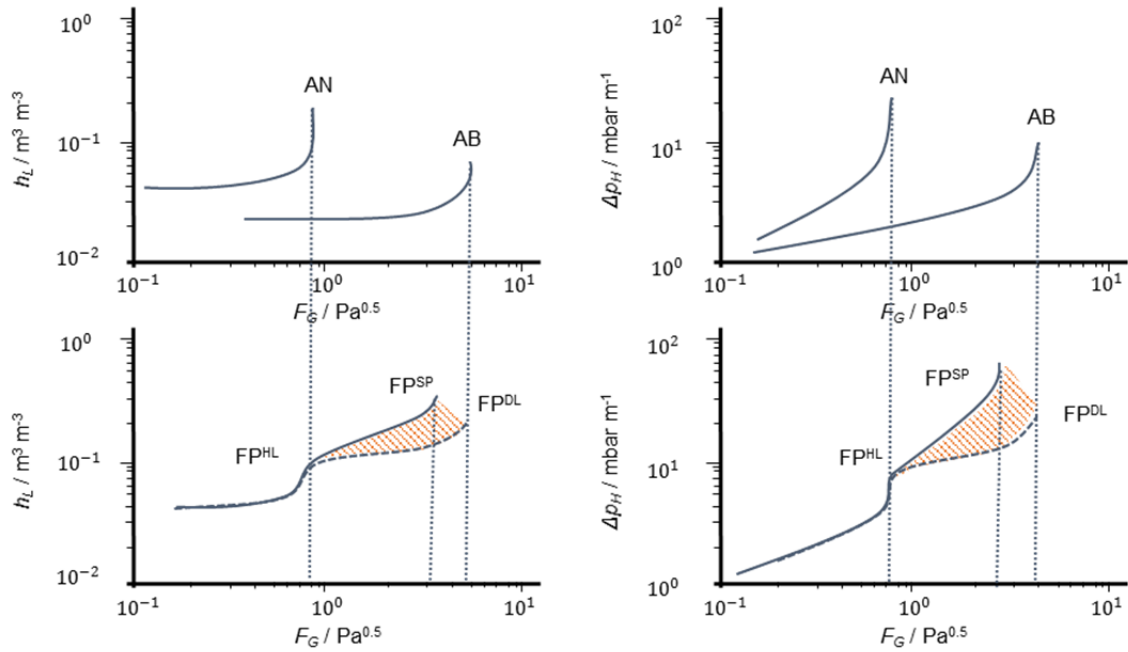


Figure 1: Relationship of the holdup (a,c) and pressure drop (b,d) between conventional structured packings (a,b) and SPs (c,d).

2. Experimental investigations

CO₂ absorption experiments with sandwich packings were carried out in a pilot-scale absorption/desorption plant schematically presented in Figure 2. The major parts of the plant are the DN 100 absorption column with a height of 3.2 m and the DN 300 desorption column with the same height. The raw gas is saturated with water before entering the absorption column, to guarantee consistent experimental conditions. In the washing section after the absorption column, the gas is purified from amines by water. The plant has several storage tanks for the loaded or uncharged solvents. In addition, the desorbed CO₂ can be recycled and stored. The temperatures of the gas and liquid inlet of the absorption column can be varied in the range from 20 to 40 °C using different heat exchangers. Specific liquid loads between 10 m³/(m²h) and 60 m³/(m²h) can be adjusted and the F-factor can be changed between 0.5 Pa^{0.5} and 4 Pa^{0.5}. By using multiple sampling devices, concentration profiles of gas and liquid phase as well as temperature profiles of the gas phase can be measured along the columns. Detailed information on the experimental setup and the used procedures can be found in Hüser and Kenig (2014).

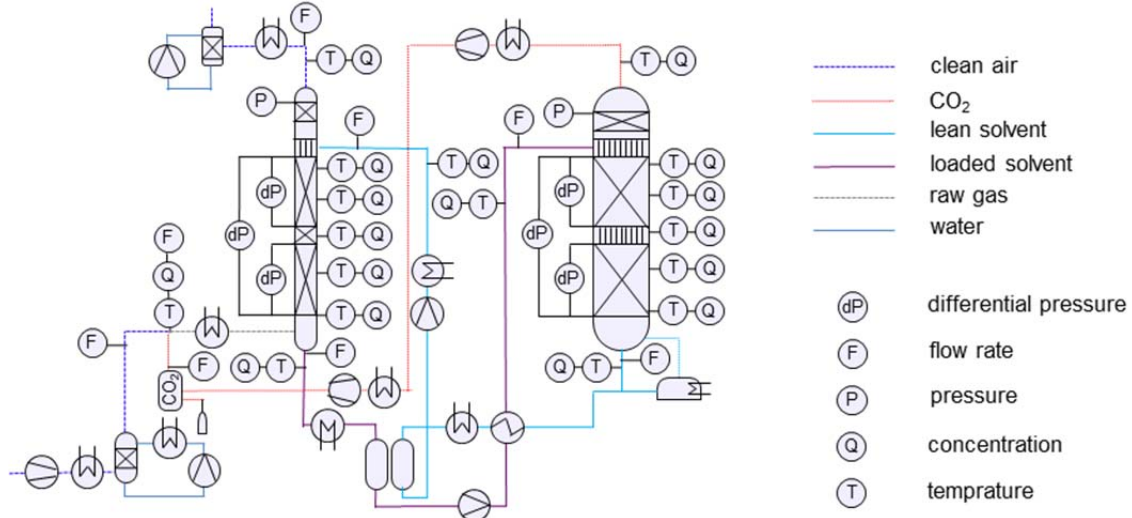


Figure 2: Schematic diagram of the pilot-scale absorption/desorption plant

The CO₂ absorption by aqueous MEA solutions in SPs was studied in the plant described above. The experimental conditions of the test series are listed in Table 1. In the packed section of the column, 13 DL with 19.6 cm height each and 12 HL with 5.0 cm height each were installed. The impact of the HL specific surface area on the separation characteristics was investigated. Besides, the flow rates of both phases, concentrations of the solvent as well as the raw gas concentration were varied. In these test series, the influence of the most important operating parameters on the CO₂ absorption was considered. The measured data provide a basis for the model validation.

Table 1: Experimental conditions

Experiment	Montz-pack combination	h_{HL}	$y_{CO_2,in}$	$X_{CO_2,in}$	u_L	$T_{G,in}$	$T_{S,in}$	F_G	w_{MEA}	CO ₂ removal efficiency, %
1	B1-750 / B1-250	50	0.0554	0.2637	40.6	31.0	38.6	1.4	0.18	79.5
2	B1-750 / B1-250	50	0.0530	0.2737	40.6	30.7	38.6	0.8	0.18	91.0
3	B1-750 / B1-250	50	0.1299	0.2604	25.5	30.6	39.5	1.4	0.17	43.2
4	B1-750 / B1-250	50	0.0556	0.2496	25.5	32.2	39.4	1.4	0.18	75.3
5	B1-750 / B1-250	50	0.1234	0.2193	25.5	31.1	39.5	1.4	0.30	79.5
6	B1-750 / B1-250	50	0.0877	0.2347	25.5	31.5	39.5	1.4	0.29	79.2
7	B1-750 / B1-250	50	0.0517	0.2843	25.5	30.8	38.5	1.4	0.28	75.8
8	B1-750 / B1-250	50	0.0893	0.2647	40.6	31.0	38.6	1.4	0.29	85.8
9	B1-1000 / B1-250	50	0.0516	0.2182	40.5	29.5	40.2	1.5	0.18	86.2
10	B1-500 / B1-250	50	0.0554	0.2681	40.5	30.6	38.1	1.4	0.18	75.1

3. Rate-based stage modelling concept for SPs

Tray and packed columns can be described using a modelling concept based on stages. Here, the column is subdivided onto alternating segments (stages). A reliable method for the description of absorption units is given by the rate-based concept, which uses the two-film theory of Lewis and Whitman (1924). In a recent publication, Hüser et al (2017) applied a validated rate-based model to describe CO₂ absorption columns with structured packings, in which MEA and AMP were used as solvents. In our work, this model is extended to take the different flow patterns evolving in SPs into account.

The reactions accompanying the absorption of CO₂ by aqueous MEA solutions can be characterized by the two-step mechanism, whereby the amines react with CO₂ forming a zwitterion as an intermediate (Vaidya and Kenig, 2007). The whole reaction system includes a set of five parallel and consecutive reactions in the liquid phase; two of them are kinetically controlled, reversible and three are instantaneous, reversible (Kucka et al., 2003). The liquid phase contains both molecular and electrolyte species. Therefore, the electrolyte-non-random two-liquid (eNRTL) model is used to consider the non-idealities in the thermodynamic equilibrium.

Due to the complexity of the flow in SPs, different options for the application of the rate-based concept to SPs can be applied. Brinkmann et al. (2009) suggested the first approach towards determination of the performance characteristics of SPs. For a SP element, the correlations of Billet and Schultes (1999) developed for structured and random packings were applied to estimate mass transfer coefficients and interfacial area in the HL and DL. Yildirim and Kenig (2015) proposed a more detailed modelling method, in which the packed sections of the column was subdivided onto two alternating segments, in line with the structure of the SP. Mass transfer coefficients and interfacial area for the DL were also estimated with correlations by Billet and Schultes (1999) valid for conventional structured packings. For the HL, however, an analogy to the flow on sieve trays was assumed, and hence, correlations for sieve trays proposed by Zuiderweg (1982) were adjusted.

A physically more consistent modelling approach should be able to consider all flow regimes depending on the operating range of SPs (cf. Figure 3). The prevailing flow regimes can change along the height of a SP element as a function of the F-factor. As a result, three different fluid dynamic ranges are defined, in which SPs can be operated. In the first range, SPs operate like conventional structured packings, while film-like flow pattern prevails in both layers. In this operating range, both the HL and the DL can be described with correlations for conventional structured packings. In our work, the correlations proposed by Olujic et al. (2004) are used for segments, in which film flow is dominating. The height of the two segments is determined by the height of the used packing layers. In the range between the loading point and flooding point of the HL, an enormous rise of both holdup and pressure drop is observed. This rise of pressure drop and holdup indicates that the flow pattern in a SP element changes and the flooded proportion in the HL grows.

Tomographic measurements showed that the flow behaviour of both the flooded HL and the froth sub-layer is similar. Furthermore, the values of liquid holdup in both layers were almost the same (Sohr et al., 2017). Consequently, it is assumed that the flooded HL can be modelled like the froth sub-layer within the DL. Therefore, the interfacial area and the mass transfer coefficients of the flooded volume in the HL are determined with correlations for sieve trays, as suggested by Yildirim and Kenig (2015). For the film-like flow patterns in the HL and in the DL, again, correlations valid for structured packings are used. The determination of the two segment heights in the HL depends on the HL entire height and the height of the flooded volume in the HL. For the froth in the HL, it is assumed that its height can be linearly interpolated between the values at the loading point and the flooding point of the HL.

In the range, in which SPs are normally operated, a froth sub-layer is formed within the DL. For froth segments in both the DL and the HL, correlations for sieve trays are applied and the film flow in the DL is described with correlations for packed columns. The height of the froth segment in the HL is equal to the entire HL height. The height of the froth sub-layer in the DL is calculated by an empirical correlation, which mirrors the dependence of the velocities of both phases, geometrical parameters of SPs and material properties (Flechsigt et al. 2016). The height of the film-like pattern segment in the DL is equal to the entire height of the DL minus the height of the froth sub-layer.

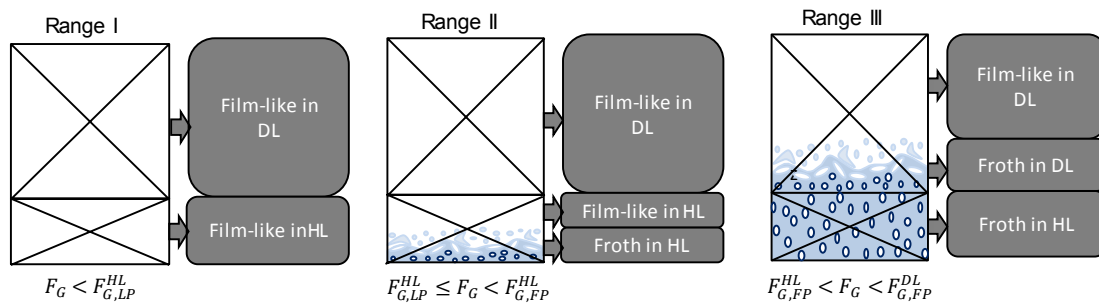


Figure 3: Arrangement of the modelling segments depending on the prevailing flow regimes

In general, the quality of rate-based stage models is strongly influenced by a proper prediction of the model parameters, namely pressure drop, holdup, mass transfer coefficients and interfacial area. Especially for SPs, a high accuracy of the description of fluid dynamics is required. In particular, a precise prediction of the flooding points is essential in order to determine correctly the operating range and the corresponding heights of each segment. In our work, the flooding points of SPs are calculated with the aid of the Wallis plot (Wallis, 1969). The Wallis plot is an approach to provide an empirical flooding point correlation based on experimental data, which was applied by Yildirim et al. (2015) for the determination of the SPs loading limits. For pressure drop calculations within our model, an additive approach for SPs proposed by Brinkmann et al. (2012) is used. In this approach, the prediction of pressure drop is based on the fluid dynamic model for packed columns suggested by Maćkowiak (2010). Flechsigt et al. (2016) extended the additive approach towards holdup determination and provided a new correlation for the estimation of the froth height in the DL.

4. Results

Simulations were carried out based on the modelling concept described above. The model was implemented in the commercial software Aspen Custom Modeller® (ACM, see www.aspentech.com). The inlet conditions and the configuration of the column were set in accordance with the experimental setup shown in Section 2 (cf. Table 1). It is important to use mass transfer coefficients and interfacial area correlations consistently; therefore, certain adjustments were necessary. Recent tomographic investigations of structured packings demonstrate, in contrast to the previously published data, that there is no total wetting of the packing surface for aqueous solutions, even at high liquid loads (Schug and Art, 2016). Consequently, we assume that previous interfacial area correlations for structured packings overestimate the reality. Therefore, the correlation applied in this work was adapted. For this purpose, we performed rate-based simulations with conventional structured packings. Afterwards, the mass transfer coefficients were adjusted in order to obtain an agreement with experimental data published by Notz et al. (2012). From the recent tomographic measurements of the interfacial area of the froth in SPs, the value range of the interfacial area is known. As a result, the interfacial area correlation suggested by Yildirim and Kenig (2015) was also adapted using a correction factor. Regarding the mass transfer coefficients in the froth, we assume that their values are either slightly higher or in the same value range as values of the mass transfer coefficients for rivulet flows. The applied correction factors for the adjustments of the model parameters are shown in Table 2.

Table 2: Applied correction factors

Flow regime	Correlation	Factor for k_G	Factor for k_L	Factor for a_{int}
Film-like pattern and rivulets	Olujic et al. (2004)	6	14	0.65
Froth regimes	Yildirim and Kenig (2015)	2.25	13	0.56

To test the numerical grid independence of the simulation results, the number of stages along the column axis and the number of the grid points of the liquid film were varied. In SPs, the lowest possible number of stages is related to the number of fluid dynamic regimes. In the considered case, the column was filled with 12 SP elements plus one DL. Therefore, 12 elements times three regimes plus one DL resulted in 37 stages for this configuration. It was revealed that the axial discretization due to this segmentation is sufficiently accurate. With the non-equidistant discretization of the liquid film in radial direction, six grid points were enough to obtain grid independence.

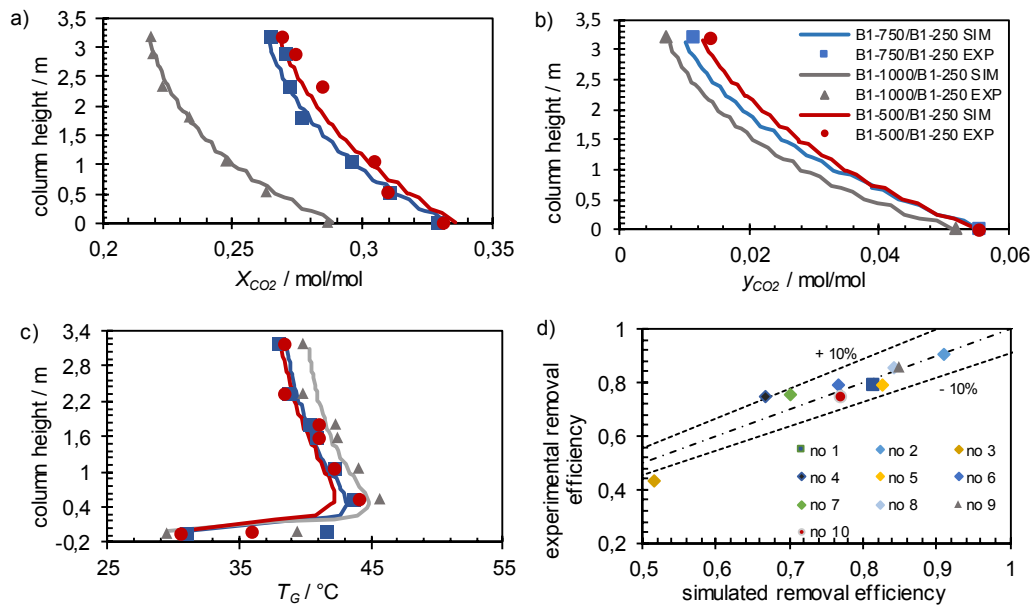


Figure 4: Column profiles of the liquid-phase loading in mol CO_2 /mol MEA (a), molar fraction of CO_2 in the gas phase (b), gas temperature (c) and parity plot of the experimental removal efficiency against the simulated values (d)

Experimental data and simulation results were plotted as column profiles of the CO_2 concentrations in both phases and the gas temperature (cf. Figure 4a-c). Here, the impact of the HL specific surface area in the operating range between the flooding points of both layers is presented. In Figure 4b, it is shown that with growing HL specific surface area the outlet concentration of the CO_2 in the gas phase drops, and thus, the mass transfer efficiency is enhanced as expected. The inlet liquid-phase loading of CO_2 is lower for the investigations with the HL B1-1000 (cf. Figure 4a), which means that the potential for the CO_2 absorption is somewhat higher. Therefore, a bigger change between the inlet and outlet liquid-phase loadings of CO_2 for the B1-1000 / B1-250 is visible compared to those of the two other SP combinations. This bigger change causes a higher temperature rise in the column (cf. Figure 4c). In addition to the capability to capture the impact of the HL specific surface area, the model shown in Section 4 can reproduce the influence of different operating parameters on the CO_2 absorption performance (Figure 4d).

5. Conclusions

In this work, the performance characteristics of CO_2 absorption columns containing SPs was studied using both experimental and theoretical investigations. The CO_2 absorption in aqueous MEA solutions was measured in a pilot-scale absorption/desorption plant. The rate-based model covering the different regimes in the different operating ranges of SPs was developed. Since different contributions of the different fluid dynamic regimes on the mass transfer are expected, each fluid dynamic regime is considered separately by appropriate correlations. The column is subdivided onto alternating segments in accordance with the

prevailing flow pattern. Experimental data were used to validate the model. It was shown that the model is capable of predicting the separation efficiency with an accuracy of 10 %.

Acknowledgments

The authors are grateful to the German Research Foundation for the financial support (DFG KE 837/26-1, HA 3088/10-1).

Notation

a_{int}	Interfacial area [m^2/m^3]	X_{CO_2}	Liquid phase loading [mol_{CO_2}/mol_{MEA}]
F_G	F-factor [$Pa^{0.5}$]	y_{CO_2}	Molar fraction [mol/mol]
h_L	Holdup [m^3/m^3]		
$k_{G/L}$	Mass transfer coefficients [m/s]		Abbreviations
Δp_H	Specific pressure drop [$mbar/m$]	DL	De-entrainment layer
$T_{G,in}$	Gas inlet temperature [$^{\circ}C$]	HL	Holdup layer
$T_{S,in}$	Solvent inlet temperature [$^{\circ}C$]	FP	Flooding point
u_L	Specific liquid load [$m^3/(m^2h)$]	LP	Loading point
w_{MEA}	Mass fraction [mol/mol]	SP	Sandwich packing

References

- Billet R., Schultes M., 1999, Prediction of mass transfer columns with dumped and arranged packings: update summary of the calculation method of Billet and Schultes, *Chemical Engineering Research and Design*, 77, 498-504.
- Brinkmann U., Hoffmann A., Kaibel B., Jödecke M., Kenig E.Y., 2009, Ein rate-based Ansatz zur Berechnung der Trennleistung von Anstaupackungen, *ProcessNet Conf. on Fluid Process Engineering*, Dortmund.
- Brinkmann U., Kaibel B., Jödecke M., Mackowiak J., Kenig E.Y., 2012, Beschreibung der Fluidodynamik von Anstaupackungen, *Chemie Ingenieur Technik*, 84, 36–45.
- Flechsig S., Yildirim Ö., Kenig E.Y., 2016, Sandwich packings: State of the art, *ChemBioEng Reviews*, 3, 174-185.
- Hüser N., Kenig E.Y., 2014, A new absorption-desorption pilot plant for CO₂-capture, *Chemical Engineering Transactions*, 39, 1417-1422.
- Hüser N., Schmitz O., Kenig E.Y., 2017, A comparative study of different amine-based solvents for CO₂-capture using the rate-based approach, *Chemical Engineering Science*, 157, 221-231.
- Kashani N., Siegert M., Sirch T., 2005, A new kind of column packing for conventional and reactive distillation – the Sandwich packing, *Chemical Engineering and Technology*, 28, 549-552.
- Kucka L., Müller I., Kenig E.Y., Górak A., 2003, On the modelling and simulation of sour gas absorption by aqueous amine solutions, *Chemical Engineering Science*, 58, 3571–3578.
- Lewis W. K., Whitman W. G., 1924, *Principles of Gas Absorption*, *Ind. Eng. Chem.*, 16, 1215-1220.
- Maćkowiak J., 2010, *Fluid Dynamics of Packed Columns*. Springer-Verlag, Berlin.
- Notz R., Mangalapally, H.P., Hasse H., 2012. Post combustion CO₂ capture by reactive absorption: Pilot plant description and results of systematic studies with MEA, *Int. J. Greenhouse Gas Control*, 6, 84-112.
- Olujic Z., Behrens M. Colli L., Paglianti A., 2004, Predicting the efficiency of corrugated sheet structured packings with large specific surface area, *Chemical and Biochemical Engineering Quarterly*, 18, 89-96.
- Schug S., Artl W., 2016, Imaging of fluid dynamics in a structured packing using X-ray computed tomography, *Chemical Engineering and Technology*, 39, 1561-1569.
- Sohr J., Litzka A., Schubert M., Flechsig S., Kenig E.Y., Hampel U., 2017, Untersuchung heterogener Strömungsmuster in Anstaupackungen mittels ultraschneller Röntgentomografie, *ProcessNet Conf. on Fluid Process Engineering*, Köln.
- Vaidya P. D., Kenig E.Y., 2007, CO₂-alkanolamine reaction kinetics: A review of recent studies, *Chemical Engineering and Technology*, 30, 1467-1474.
- Wallis G. B., 1969, *One-Dimensional Two-Phase Flow*, McGraw-Hill, New York.
- Yildirim Ö., Flechsig S., Brinkmann U., Kenig E.Y., 2015, Application of the Wallis plot for the determination of the loading limits of structured packings and sandwich packings, *Chemical Engineering Transactions*, 45, 1165-1170.
- Yildirim Ö., Kenig E.Y., 2015, Rate-based modelling and simulation of distillation columns with sandwich packings, *Chemical Engineering and Processing*, 98, 147-154.
- Zuiderweg F.J., 1982, Sieve trays: a view on the state of the art, *Chemical Engineering Science*, 37, 1441-1464.